Micellization Behavior of $PS(PI)_3$ Miktoarm Star Copolymers

Kondylia Sotiriou, Aspasia Nannou, Gabriel Velis, and Stergios Pispas*

Department of Chemistry, University of Athens, Panepistimiopolis Zografou, 15771 Athens, Greece

Received October 15, 2001; Revised Manuscript Received January 30, 2002

ABSTRACT: We present light scattering and viscometric results from micellar solutions of $PS(PI)_3$ 4-miktoarm stars (i.e. stars with chemically different arms) in two selective solvents, *n*-decane (selective for PI) and dimethylacetamide (DMA, selective for PS), for the different arms. A series of samples having different molecular weights and compositions were investigated in order to determine the influence of these molecular parameters as well as that of molecular architecture in the micellization behavior. Experimental results indicate that spherical micelles are formed in *n*-decane, a selective solvent for polyisoprene. Aggregation numbers and hydrodynamic radii of the micelles increased with increasing molecular weight and content of the insoluble component. The area of the core-corona interface per copolymer chain, A_c, was found to increase compared to the diblock case due to crowding of the three PI arms in the corona. In DMA, experimental evidence exists that points to the formation of nonspherical micelles. Aggregation numbers in this solvent are larger than *n*-decane. Polydispersity of the micelles is also increased. Experimental findings are discussed taking into account solvent selectivity and molecular architecture of the miktoarm stars.

Introduction

The micellization of block copolymers in selective solvents has attracted the interest of scientists for some decades now.[1,2] This is due to the great potential of this kind of supramolecular structure for use in a diverse field of practical applications including stabilization of colloidal dispersions, controlled drug delivery, removal/recovery of organic compounds from contaminated water, catalysis in micellar nanoreactors, cosmetics etc.[3,4] Micelle formation is driven by the unfavorable interactions between the selective solvent and the insoluble blocks of the copolymer which tent to associate in order to decrease these interactions. The dependence of the structural parameters of micelles on the molecular characteristics of block copolymers has been studied in detail both experimentally[5−11] and theoretically.[12−15] Other factors affecting micelle formation and structure including copolymer concentration, temperature, and solvent selectivity were also addressed in the literature. The influence of the macromolecular architecture on the micellization process in general is a less studied field since well defined, architecturally complex, block copolymers have been synthesized only recently.[16−23]

In this paper, we report results on the micellization properties of a series of $PS(PI)_3$ 4-miktoarm star copolymers (i.e. 4-arm stars having one PS arm and three PI arms) in two selective solvents: *n*-decane, which is a selective solvent for polyisoprene (PI), and dimethylacetamide (DMA), which is a selective solvent for polystyrene (PS). Static and dynamic light scattering as well as dilute solution viscometry, were used in order to determine aggregation numbers, size, shape, and polydispersity of the micelles in each case. The major goal of this work is to study the influence of macromolecular architecture, in relation to other molecular chararacteristics of the miktoarm stars, and of solvent selectivity on the primary characteristics of the micelles formed.

Experimental Section

Polymer Synthesis. All samples were synthesized by anionic polymerization high vacuum techniques.[24] The $PS(PI)_3$ miktoarm stars were prepared by reaction of the single living arm (PS) with an excess of $SiCl_4$ to produce the trifunctional chlorosilane end-capped macromolecular agent. After removal of the $SiCl_4$ excess on the vacuum line, a stoichiometric excess of the second arms (PI) was added. When the coupling reaction was completed, as evidenced by SEC analysis, the excess of the second arm was deactivated with methanol. The desired $PS(PI)_3$ 4-miktoarm stars were isolated from the reaction mixture by solvent/nonsolvent fractionation (toluene/methanol). The pure miktoarm stars were rigorously characterized by size exclusion chromatography with RI and UV detection, membrane osmometry, LALLS, and ^{1}H NMR in order to provide the molecular characteristics of the materials. These measurements confirmed the high degree of compositional, molecular weight, and architectural homogeneity of the copolymers. Details on the synthesis and the molecular characterization of the miktoarm stars were given elsewhere.[25,26] The molecular characteristics of the samples under study are given in Table 1. They can be grouped into two series according to the overall molecular weight: the high molecular weight series (samples 4IS60, 4IS40, 4IS35, and 4IS13) and the low molecular weight series (samples 4IS33, 4IS65, and 4IS25), where the code numbers denote the approximate PI content of each sample.

Micellization Studies. Analytical grade *n*-decane and DMA were first dried over CaH_2 under reflux for 24h. Both solvents were fractionally distilled just before use. Stock solutions were prepared by dissolving the appropriate amount of sample in the corresponding volume of dried solvent. The solubility parameters for the solvents and the polymeric blocks are (in $(cal/cm)^{1/2}$): $\delta_{PS} = 9.1$, $\delta_{PI} = 8.1$, $\delta_{n-decane} = 6.6$, $\delta_{DMA} = 10.8$.[27] These values indicate that both solvents are about equally bad solvents for the insoluble arms and of about equal quality for the soluble arms.

The samples having the lower overall molecular weights and compositions of the insoluble part dissolved in the selective solvents at room temperature after 24 h. Samples having high molecular weights and content of the insoluble part had to be heated at 70 °C for some hours in order to be dissolved completely, especially in the case of *n*-decane. Generally, dissolution in DMA was easier. This can be attributed to the lower T_g of PI, which makes dissolution in a selective solvent easier in the second case. The stock solutions were heated at 70 °C for an additional 2 h period before the measurements, to ensure complete dissolution of the samples and removal of

10.1021/ma011795c CCC: $22.00
Published on Web 04/04/2002

Table 1. Molecular Characteristics of the PS(PI)$_3$ Miktoarm Star Copolymers

sample	M_n[a] × 10^{-3}	M_w[b] × 10^{-3}	M_w/M_n[c]	M_w/M_n[d]	%wt PS[e]	$M_{n,PS}$[a] × 10^{-3}	$M_{n,PI}$[a] × 10^{-3}	N_{PS}[f]	N_{PI}[f]
4IS60	77.2	80.1	1.05	1.04	43	35.2	14.5	338	213
4IS40	104	108.3	1.04	1.04	60	59.3	14.2	570	209
4IS35	92.3	97.3	1.03	1.05	65	59.3	11.7	570	172
4IS13	199	204	1.03	1.02	88	180	7.6	1731	112
4IS33	11.5	12.2	1.04	1.06	62	7.7	1.6	74	24
4IS65	24.0	25.1	1.04	1.04	34	7.7	6.5	74	96
4IS25	22.0	22.9	1.04	1.04	71	16.3	1.9	157	28

[a] By membrane osmometry in toluene. [b] By LALLS in THF. [c] By SEC in THF. [d] By LALLS and osmometry. [e] By ^{1}H NMR in $CDCl_3$. [f] Degrees of polymerization of PS and PI arms.

Table 2. Results on PS(PI)$_3$ Miktoarm Star Micelles in *n*-Decane at 25 °C

sample	M_w × 10^{-6}	A_2 × 10^4	N_w	$D_{o,app}$ × 10^8 (cm^2/s)	k_D	R_h (nm)	[η] (mL/g)	k_H	R_v (nm)
4IS60	2.7	0.12	34	11.8	2.8	20.2	18.6	1.6	20.0
4IS40	19.3	~0	178	8.55	12	28	11.2	1.3	32.5
4IS35	50.0	~0	514	10.5	20	34.4	8.9	1.7	41.3
4IS33	0.28	−1.50	23	23.6	5	10.2	6.4	0.9	6.6
4IS65	0.029	2.24	1	50.5	14	4.8	15.4	1.05	4.1
4IS25	1.9	~0	83	17.2	68	13.9	6.0	1.3	12.2

possible memory effects.[3] Memory effects are expected to be more important in the case of *n*-decane due to the high T_g of PS, whereas the low T_g of PI ensures a micellar structure closer to equilibrium. Using the above sample preparation protocol, reproducible results were obtained by all methods from different determinations on the same sample. No polymer precipitation was observed from these solutions after standing at room temperature for several weeks. Solutions of lower concentrations were obtained by subsequent dilutions of the stock solutions. Before light scattering measurements, the solutions were filtered through 0.45-μm nylon filters, whereas for viscosity measurements, 1.2-μm nylon filters were used. Measurements by the different methods were carried out in the broader concentration range possible taking into consideration experimental limitations. All measurements were performed at 25 °C.

Apparent weight average molecular weights, M_w, of the micelles and second virial coefficients, A_2, in *n*-decane were obtained from the linear part of the concentration dependence of the reduced scattering intensity at high concentrations, using a Chromatix KMX-6 low-angle, laser-light-scattering photometer operating at 633 nm. Additional measurements were made at different angles for the determination of the apparent radius of gyration, R_g, using a Series 4700 Malvern system composed of a PCS5101 goniometer interfaced with a PCS7 stepper motor controller and a Cyonics variable power Ar^+ laser operating at 488 nm. The required specific refractive indices, d*n*/d*c*, were obtained at 633 nm by a Chromatix KMX-16-laser differential refractometer and at 488 nm by an Optilab DSP (Wyatt Technology) interferrometric refractometer, both calibrated with NaCl standard aqueous solutions. d*n*/d*c* values for the samples were in the range 0.146 to 0.154 in *n*-decane and 0.123 to 0.144 in DMA, depending on composition and molecular weight. These high values allow the determination of the M_w of the micelles with reasonable accuracy. Additionally, due to the low compositional heterogeneity of the samples, the determined M_ws must be close to the true ones.

Dynamic light scattering experiments were carried out using the same Malvern system operating in the dynamic mode. A 192-channel correlator was used for accumulation of the data. Correlation functions were analyzed by the cumulant method. The Contin software was provided by the manufacturer. The correlation functions were collected at angles between 45° and 135°. Apparent diffusion coefficients at zero concentration, $D_{o,app}$, were obtained after extrapolation to zero angle by the use of eq 2:

$$D_{app} = D_{o,app}(1 + k_D c) \quad (1)$$

where D_{app} is the diffusion coefficient measured at each concentration and k_D the coefficient at the concentration dependence of D_{app}. Apparent hydrodynamic radii, R_h, were determined by the equation

$$R_h = k_B T/6\pi\eta_o D_{o,app} \quad (2)$$

where k_B is the Boltzmann constant, T the absolute temperature, and η_o the viscosity of the solvent.

For the viscosity measurements, Cannon-Ubbelohde dilution viscometers were used in a temperature controlled bath (at 25 ± 0.02 °C). Flow times for the solvent and the micellar solutions were measured with a Scott-Gerate AVS 410 automatic flow timer. Data were analyzed by means of the Huggins (3) and Kraemer (4) equations

$$\eta_{sp}/c = [\eta] + k_H[\eta]^2 c + ... \quad (3)$$

$$\ln \eta_r/c = [\eta] + k_K[\eta]^2 c + ... \quad (4)$$

where [η] is the intrinsic viscosity and k_H, k_K the Huggins and Kraemer coefficients, respectively. In some cases, a second-order fit of the data points for the Huggins equation, in terms of concentration, was used giving better agreement between the [η] values calculated by the two methods. Viscometric equivalent sphere radii, R_v, were calculated from equation

$$R_v = (3/10\pi N_A)^{1/3}([\eta]M_w)^{1/3} \quad (5)$$

where M_w is the weight average molecular weight determined by light scattering by extrapolation at zero concentration. More details on the procedures and methods used have been given elsewhere.[22,23]

Results and Discussion

Micellization Behavior in *n*-Decane. Static light scattering results for the miktoarm star micelles under investigation in *n*-decane are given in Table 2 . The M_w values determined in this solvent are larger than the ones determined in the nonselective solvent (THF), in all but one case. This suggests that all samples form multimolecular micelles except sample 4IS65. This particular sample forms unimolecular micelles in the concentration range studied (9×10^{-4} g mL$^{-1} < c < 1 \times 10^{-2}$ g mL^{-1}) as it is evident from the similar molecular weight values determined in *n*-decane and THF. In this case, the PS chain of the miktoarm must adapt a more-or-less collapsed conformation due to the poor thermodynamic quality of *n*-decane toward PS (a PS homopolymer of similar molecular weight with the

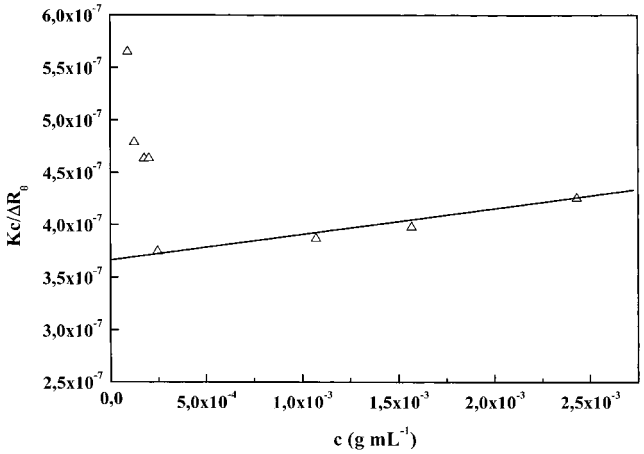

Figure 1. Static light-scattering plot showing the concentration dependence of the reduced scattering intensity for sample 4IS60 in *n*-decane. The upward curvature at the low *c* range shows coexistence of unimers and micelles as the cmc is approached.

PS arm of sample 4IS65 is insoluble in *n*-decane at 25 °C). The formation of unimolecular micelles must be a result of the macromolecular architecture alone, since a linear diblock copolymer of similar molecular weight and composition forms multimolecular micelles. A SI sample with $M_n = 29{,}000$ and 31 wt % PS forms micelles with $N_w = 248$.[6] This is an indication that the presence of three PI chains per PS chain increases the solubility of the whole macromolecule.

Values of the second virial coefficient are low due to the high molecular weight of the micelles and/or the unfavorable thermodynamic interactions between solvent and macromolecules. The aggregation numbers follow the trend known from diblock copolymers[1,2] i.e., they increase as the molecular weight of the miktoarm star copolymers increases at similar composition (e.g. samples 4IS35 and 4IS33 in Table 2) and as the molecular weight of the insoluble block increases at constant length of the soluble blocks (samples 4IS60 and 4IS40, and 4IS25 and 4IS33 in Table 2). On the other hand, at constant length of the insoluble arm, aggregation number increases as the length of the soluble arm decreases (samples 4IS40 and 4IS35, and 4IS65 and 4IS33). Attempts made to determine the critical micelle concentration, by extending the measurements at the lowest concentrations possible, were unsuccessful. It seems that the cmc in the cases studied is very low. In some cases, light scattering plots show an upturn at low *c* (Figure 1) indicative of the proximity to the cmc.

A comparison of the aggregation numbers determined for the 4-miktoarm stars with linear diblock copolymers aggregation numbers from the literature clearly shows the effect of architecture i.e., a decrease in the aggregation number of the micelles formed by the nonlinear block copolymers is observed as it was also observed in other cases of nonlinear block copolymers.[16−23] For example, comparison of samples 4IS60 and 4IS40 with samples SA-4 and SA-7 of ref 6 shows that the miktoarm micelles have a lower aggregation number despite the fact that the overall molecular weight of the miktoarms is almost double that of the linear diblocks. Additionally, a SI sample having $M_w = 24{,}000$ and 75 wt % PS, studied in the course of this work, shows an aggregation number equal to 980, whereas sample 4IS25, having similar molecular characteristics, shows an N_w equal to 83, at the same concentration range in *n*-decane.

Table 3. Structural Parameters for PS(PI)$_3$ Miktoarm Star Copolymer Micelles in *n*-Decane

sample	R_v/R_h	L_{corona} (R_h-R_c)	R_c (nm)	A_c (nm^2)
4IS60	0.99	12.6	7.6	21
4IS40	1.16	11.6	16.4	18.8
4IS35	1.2	11.3	23.1	11.2
4IS33	0.65	6.2	4.0	10.6
4IS65[a]	0.80	-	-	-
4IS25	0.88	5.9	8	9.7

[a] This sample forms unimolecular micelles in the concentration range studied.

Obviously, the additional geometrical and spatial constraints that exist during the incorporation of a PS(PI)$_3$ molecule in a micelle are responsible for the observed behavior.

The conclusions drawn from static light scattering are supported by dynamic light scattering measurements (Table 2). The R_h values are high, indicating association and they increase as the aggregation number of the micelles increases. The R_h value for the unimolecular micelles formed in solutions of sample 4IS65 is also given. k_D values do not show a definite trend since hydrodynamic and thermodynamic interactions may cancel each other as a result of the association process. Analysis of the intensity correlation functions by the method of cumulants and Contin reveals that the micelles formed are almost monodisperse in size. The ratio μ_2/Γ^2 is less than 0.1 from cumulants analysis, where μ_2 is the second cumulant and Γ is the decay rate of the correlation function. Whereas Contin analysis shows only one narrowly distributed peak at the high concentration range, where micelles are the dominant species in solution. In some cases, at lower concentrations two peaks could be resolved corresponding to unimers and micelles coexisting in solution (especially in the case of the low molecular weight samples). The results are in accordance to the model of closed association,[1−3] where unimers and micelles having a well-defined aggregation number are in equilibrium, the later being shifted in favor of the micelles as the concentration of the copolymer increases.

More information on the micellar characteristics can be drawn from viscometry. The results are also shown in Table 2. [η] values are rather low if one takes into account the high molecular weight of the multimolecular micelles. k_H values are increased due to increased hydrodynamic interactions between chains incorporated in micelles. In most cases, k_H is larger than 0.99, the value for hard spheres[28] (some theories give even lower k_H values for hard spheres). Both experimental findings tend to the conclusion that the micelles formed in this solvent have a rather compact structure. It is worth mentioning that k_H is also high in the case of the unimolecular micelles of sample 4IS65. Evidently, the collapse of the insoluble block, as a result of a thermodynamically poor environment, and the conformation of all blocks in the unimolecular micelle, favor the increase of hydrodynamic interactions between segments.[1−3] Apparently, the conformation of the particular miktoarm star molecule in *n*-decane is more compact than that in a good solvent for both blocks.

Table 3 summarizes the structural characteristics of the micelles formed by the PS(PI)$_3$ miktoarm stars in *n*-decane. The ratio R_v/R_h is close to unity, within experimental error, in most cases indicating a spherical shape for the micelles.[8,28,29] This is also expected from the internal symmetry of these type of macromolecules.

Scheme 1

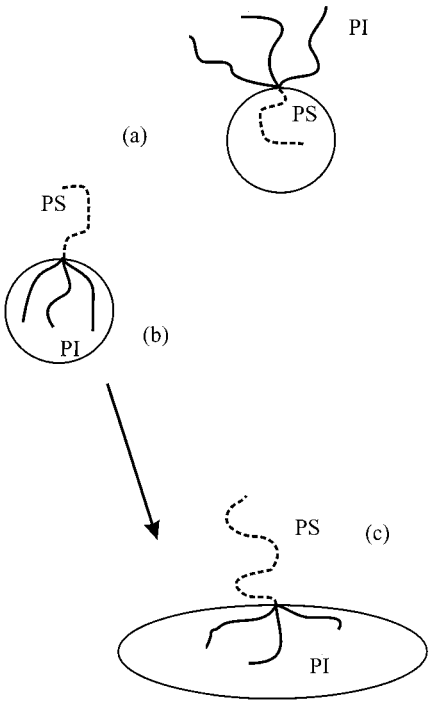

As depicted in Scheme 1a, there is a tendency of the interface to be curved toward the PS arm due to the presence of three PI arms connected to the common branching point, which is on the same direction as the curvature induced by the formation of the micellar core in *n*-decane. The radius of the micellar core, R_c, the area per branching point, A_c, and the width of the micellar corona, L_{corona}, were calculated by aid of the following equations:

$$R_c = (3M_{w,mic}\, wt_{PS}/4\pi N_A d_{PS}\phi_{PS})^{1/3} \quad (6)$$

$$A_c = 4\pi R_c^2/N_w \quad (7)$$

$$L_{corona} = R_h - R_c \quad (8)$$

and are also presented in Table 3. In equations (6−8), N_A is the Avogadro number, wt_{PS} is the weight fraction of PS in the copolymer, d_{PS} is the density of pure PS ($d_{PS} = 1.05$ g mL^{-1}), and ϕ_{PS} the volume fraction of PS in the core. The assumption of a dry PS core ($\phi_{PS} = 1$) was made. This is not an entirely unrealistic assumption, since *n*-decane is a bad solvent for PS. Even if a small swelling of the core takes place, it would not considerably alter the conclusions drawn because the calculated values would, in any case, be within the experimental error of the determinations of the parameters used for the calculations. The results indicate that R_c depends on the molecular weight of the PS arm and the aggregation number as expected.[1−3] A_c does not have a constant value, but depends on the molecular weight of the PI arm (and the aggregation number). A similar dependence is also obvious for L_{corona}. Compared to the diblock case,[6,22] A_c values for the PS(PI)$_3$ miktoarms are larger. This can be expected since in the PS(PI)$_3$ case, three PI arms are connected to the same point at the core-corona interface and crowding effects are active. The chains need more space in order to be confined to the area of the corona and therefore A_c increases (Scheme 1a). Comparing samples with the same PI arm molecular weight and different PS arms (e.g. samples 4IS40 and 4IS60), it is obvious that there is a small increase of L_{corona} as the length of the insoluble block as well as the aggregation number, decreases. This must be related to an increased stretching of the PI chains attached to the surface of a smaller sphere. An increase of the sphere's surface somewhat relaxes the stretching of the coronal chains.

A simple scaling analysis of the dependence of R_h of the micelles on the number of segments in the miktoarm copolymers was attempted, although the number of samples investigated is rather small. This gives a scaling relation (Figure 2a)

$$R_h \sim N_{total}^{0.52\pm0.08} \quad (9)$$

The dependence is weaker than in the case of linear diblocks where theoretical calculations agree to an exponent of around 0.68.[12−14] The weaker dependence of the size of the micelles on the total degree of polymerization is indicative of the effect of macromolecular architecture on the overall size of the micelles. The dependence of the micellar core radius on the number of PS segments seems to be $R_c \sim N_{PS}^{0.71\pm0.2}$ (Figure 2b), which is in the range predicted for diblock copolymers. This latter agreement may originate from the fact that there is only one PS chain per miktoarm molecule. Of course, the effect of a lower aggregation number for the 4-miktoarms has to be taken also into account. Similar simple calculations for the dependence of the corona thickness on the number of PI segments give $L_{corona} \sim N_{PI}^{0.24\pm0.09}$ (Figure 2c), which is also weaker than the case of diblock copolymers.[2] However, it has to be noted that for this determination the available range of data points is limited. Since the same number of corona segments are divided into three PI chains connected to the same junction point, micellar corona thickness decreases compared to a diblock case, where only one coronal chain is present per junction point. This results in a considerable decrease of the corona thickness and the overall size of the micelles at the same total number of segments per molecule.

Micellization Behavior in DMA. The 4-miktoarm star samples were also studied in DMA. The results from static light scattering are given in Table 4. It is obvious that all samples studied form multimolecular micelles in this solvent. However, the N_w values for DMA are larger than those determined in *n*-decane. Due to the larger micelles formed in this case, determination of the radius of gyration, R_g, was possible, although these values should be used with caution, since they present apparent quantities, due to the difference in the refractive index increments for PS and PI. A_2 values are also very small in this case, for the reasons explained before.

Dynamic light scattering measurements are more revealing for the situation in the solutions in DMA (Table 4). k_D values are larger and in some cases they become negative. R_h values are also increased as a consequence of the increase in the aggregation number. Distribution analysis of the correlation functions shows somewhat increased polydispersities ($\mu_2/\Gamma^2 > 0.1$, and considerably larger in some cases), but single-peaked distributions of hydrodynamic radii are shown in the case of high molecular weight samples. In the low molecular weight series, two separate peaks could be resolved in two cases. In the case of sample 4IS33, the

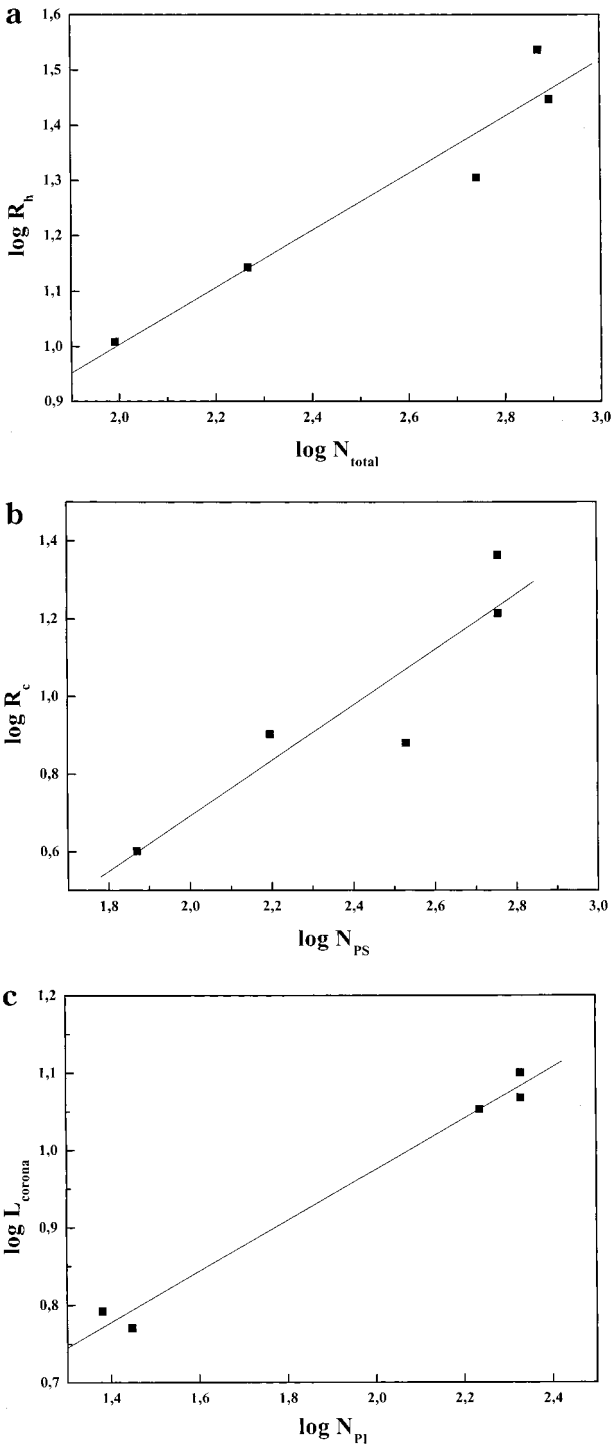

Figure 2. Scaling laws for different structural parameters of the $PS(PI)_3$ miktoarm star micelles in *n*-decane: a) log R_h of micelles vs total number of segments (N_{total}) in the copolymer, b) log R_c of micelles vs number of PS segments (N_{PS}) and c) log L_{corona} of micelles vs number of PI segments (N_{PI}).

low R_h peak can be attributed to unimers and the high R_h peak to micelles (Figure 3). The hydrodynamic radius of these micelles is larger than all other micelles investigated. Judging from the values of R_h corresponding to the peaks in the case of sample 4IS65, one can assume that they must be attributed to two kinds of micelles, since the lower R_h is too large to be ascribed to free unimers. The possibilities of formation of micellar clusters or cylindrical micelles which coexist with normal micelles in solution have to be considered.[30−32] This conclusion is supported by the increased polydispersity values obtained even in the case where a single peak has been resolved by Contin. We will return to this point later after examination of the viscometric results.

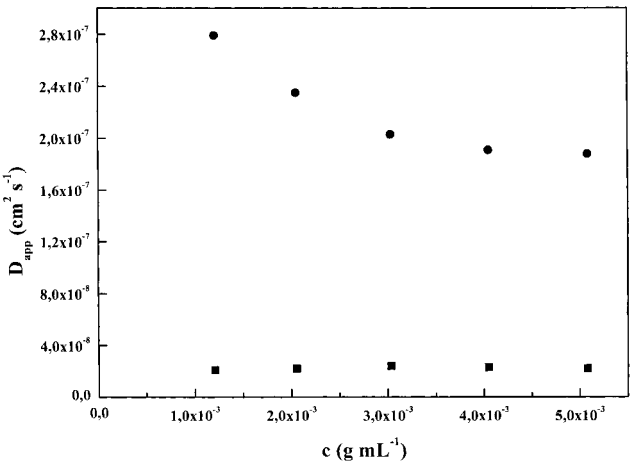

Figure 3. D_{app} vs concentration plot obtained from dynamic light scattering measurements on sample 4IS33 in DMA. Closed circles correspond to unimers and closed rectangulars to micellar clusters (or cylindrical micelles). Notice the negative slope in the unimer case, which indicates attractive interactions between unimers. D_{app} for the micellar clusters (or cylindrical micelles) shows no appreciable concentration dependence.

Viscometric results are also shown in Table 4. The [η] values are found to be substantially increased compared to those determined in *n*-decane, in the case of the high molecular weight samples (Figure 4). This may be a result of the higher aggregation number and/or the formation of supramolecular structures different than normal spherical micelles. The somewhat decreased k_H values compared to those determined in *n*-decane, point to a less compact structure for the micelles in DMA. The R_v values calculated in this solvent are larger than the R_h values in the high molecular weight samples and lower in the case of low molecular weight samples (Table 4). One has to take into account that in a capillary viscometer, shear forces are developed and some rupture of supramolecular structures is possible.[8] This should explain the low R_v/R_h ratios for the low molecular weight miktoarm micelles. A similar mechanism seems to be absent in the case of high molecular weight miktoarm micelles. In the latter case, the PI arms are larger than the entanglement length of this polymer and this may induce some resistance to rupture of the micellar cores. Additionally, due to the higher molecular weight, the cores of these micelles are expected to be more compact due to the poorer thermodynamic quality of the solvent for longer arms. The high R_v/R_h values for the high molecular weight samples may also be due to an increase in the size of the aggregates at higher concentrations (the concentrations used in viscometry are usually higher than those in light scattering). The curvature of the Huggins plots (Figure 4) points also to the same conclusion.

The possibility of a change in the shape of the micelles formed in DMA or the formation of micellar clusters can explain some of the observations. The ratio R_g/R_h has been frequently used for the elucidation of the shape and segment density profile of polymeric structures in solution.[28,33,34] The values for this ratio, where available, are larger than 0.775, the value for hard spheres,[28] and close to unity (Table 4). This experimental result points

Table 4. Results for $PS(PI)_3$ Miktoarm Star Copolymer Micelles in DMA at 25 °C

sample	$M_w \times 10^{-6}$	$A_2 \times 10^6$	N_w	R_g (nm)	$D_{o,app} \times 10^8$ (cm^2/s)	k_D	R_h (nm)	R_g/R_h	$[\eta]$ (mL/g)	k_H	R_v (nm)	R_v/R_h
4IS60	422	2.6	5268	89.4	2.54	−160	96	0.93	29.3	0.71	125	1.3
4IS40	163	5.8	1505	30.9	8.99	90.4	27.1	1.14	36.6	0.97[b]	98.1	3.6
4IS35	34	2.9	349	28.0	8.96	116.8	27.2	1.03	21.0	1.6	48.3	1.77
4IS13	18	9.0	88	30.4	7.38	8	33.0	0.92	66.9	2.02	57.6	1.75
4IS33[a]	0.28	−300	23		29	−79	8.4		9.3	0.75	7.5	-
					2.15	13	113					
4IS65[a]	2	∼0	80		2.2	153	89		18.9	0.84	18.2	-
					0.7	0	334					
4IS25	2.7	59	118		22.4	21	10.9		0.9	0.92	7.4	0.68

[a] Bimodal distribution of hydrodynamic radii. [b] A nonlinear fit gives $k_H = 0.42$ (Figure 4).

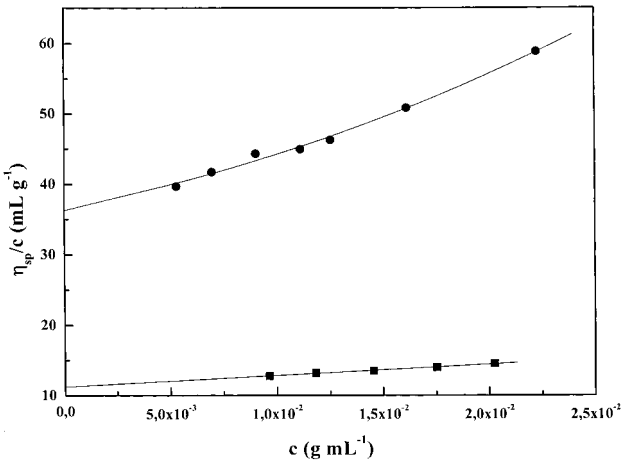

Figure 4. η_{sp}/c vs concentration plot for sample 4IS40 in *n*-decane (■) and DMA (●) at 25 °C.

toward the existence of elongated micelles in solution. One has to consider that elongated structures may be more prone to disintegration in flow fields.

From another point of view, the macromolecular structure also favors a more elongated structure as depicted in Scheme 1b−c. Formation of a PI core in DMA leads to a bending of the core-corona interface toward the three PI arms of the miktoarm copolymer. This is not a comfortable situation for the PI arms that have to be accommodated in a smaller space. A more elongated core releases some of the crowding. In this way, a more elongated structure for the whole micelle is produced. The increased R_v/R_h values in the case of the high molecular weight samples also fit to the picture of formation of elongated micelles. R_v is influenced by static structural contributions ($[\eta] \sim R_g^2 R_h$),[28] whereas R_h is a purely hydrodynamic quantity. Large R_g values are reflected in the $[\eta]$ values, which are also found to be large (Table 4), as explained before. Additionally, larger polydispersities are usually observed for elongated structures.[8]

The formation of micellar clusters cannot be entirely ruled out and micellar clustering may be mostly important in the case of micelles with poorly solvated coronas and/or having short coronal blocks and large core blocks[8,31,32] (and consequently large cores). Then, interactions between the less shielded cores or the poorly solvated coronas may lead to micellar clustering. The micelles formed by low molecular weight samples may belong to this category. This can also explain the lower R_v values compared to R_h ones. Micellar clusters may be easily broken into their constituting parts (normal spherical micelles) under shear. One can also think that formation of elongated micelles may go through the formation of micellar clusters in the initial stages of the process, followed by core fussion in the latter stages. It has to be noted, however, that clustering does not take place in *n*-decane, although this solvent is relatively poor for the PI corona blocks (judging from the difference in solubility parameters). Of course the observed complex behavior in DMA may be the result, as it is usually the case in real life, of all the aforementioned factors acting together (copolymer composition and molecular weight, miktoarm architecture and solvent quality).

Conclusions

The study of a series of well-defined $PS(PI)_3$ miktoarm stars in *n*-decane has shown that these materials form spherical micelles with narrow size distributions. The aggregation number and overall size of these micelles are smaller than the corresponding linear diblocks. Crowding of the PI arms in the micellar corona leads to increased areas on the core-corona interface per branching point. In DMA, the same materials show a complex behavior. The formation of elongated supramolecular structures or micellar clusters is supported by the experimental results at hand i.e., high aggregation numbers, large R_h and $[\eta]$ values, and increased polydispersity. The most probable cause for the observed behavior is a complex combination of macromolecular architectural effects, copolymer composition, and solvent quality. The experimental results presented may shed some light to the interplay of different factors influencing micelle formation and improve our understanding of the way polymeric supramolecular structures are constructed in solution.

Acknowledgment. The authors would like to thank Prof. N. Hadjichristidis for fruitful discussions and Dr. Y. Tselikas for help in sample synthesis.

References and Notes

(1) Tuzar, Z.; Kratochvil, P. *Surf. Colloid Sci.* **1993**, *15*, 1.
(2) Hamley, I. W. *The Physics of Block Copolymers*; Oxford University Press: Oxford, 1998.
(3) *Solvents and Self-Organization of Polymers*; Webber, S. E., Munk, P., Tuzar, Z., Eds.; NATO ASI Series, Series E: Applied Sciences, Vol. 327; Kluwer Academic Publishers: Dordrecht, 1995.
(4) (a) Forster, S.; Antonietti, M. *Adv. Mater.* **1998**, *10*, 195. (b) Antonietti, M.; Forster, S.; Oestreich, S. *Macromol. Symp.* **1997**, *121*, 75. (c) Moffit, M.; Khougaz, K.; Eisenberg, A. *Acc. Chem. Res.* **1996**, *29*, 95.
(5) Stejskal, J.; Hlavata, D.; Sikora, A.; Konak, C.; Plestil, J.; Kratochvil, P. *Polymer* **1992**, *33*, 3675.
(6) Bahadur, P.; Sastry, N. V.; Marti, S.; Riess, G. *Colloids Surf.* **1985**, *16*, 337.
(7) Oranli, L.; Bahadur, P.; Riess, G. *Can. J. Chem.* **1985**, *63*, 2691.
(8) Antonietti, M.; Heinz, S.; Schmidt, M.; Rosenauer, C. *Macromolecules* **1994**, *27*, 3276.
(9) Forster, S.; Zisenis, M.; Wenz, E.; Antonietti, M. *J. Chem. Phys.* **1996**, *104*, 9956.

(10) Calderara, F.; Riess, G. *Macromol. Chem. Phys.* **1996**, *197*, 2115.
(11) Prochaska, K.; Glocker, G.; Hoff, M.; Tuzar, Z. *Macromol. Chem.* **1984**, *185*, 1187.
(12) Noolandi, J.; Hong, K. M. *Macromolecules* **1983**, *16*, 1443.
(13) Nagarajan, R.; Ganesh, K. *J. Chem. Phys.* **1989**, *90*, 5843.
(14) Whitmoore, M. D.; Noolandi, J. *Macromolecules* **1985**, *18*, 657.
(15) Halperin, A. *Macromolecules* **1987**, *20*, 2943.
(16) Bayer, U.; Standler, R. *Macromol. Chem. Phys.* **1994**, *195*, 2709.
(17) Iatrou, H.; Willner, L.; Hadjichristidis, N.; Halperin, A.; Richter, D. *Macromolecules* **1996**, *29*, 581.
(18) Pispas, S.; Hadjichristidis, N.; Mays, J. W. *Macromolecules* **1996**, *29*, 7378.
(19) Tsitsilianis, C.; Papanagopoulos, D.; Lutz, P. *Polymer* **1995**, *36*, 3745.
(20) Voulgaris, D.; Tsitsilianis, C.; Grayer, V.; Esselink, F. J.; Hadziioannou, G. *Polymer* **1999**, *40*, 5879.
(21) Ramzi, A.; Prager, M.; Richter, D.; Efstratiadis, V.; Hadjichristidis, N.; Young, R. N.; Allgaier, J. B. *Macromolecules* **1997**, *30*, 7171.
(22) Pispas, S.; Poulos, Y.; Hadjichristidis, N. *Macromolecules* **1998**, *31*, 4177.
(23) Pispas, S.; Hadjichristidis, N.; Potemkin, I.; Khokhlov, A. *Macromolecules* **2000**, *33*, 1741.
(24) Hadjichristidis, N.; Iatrou, H.; Pispas, S.; Pitsikalis, M. *J. Polym. Sci. Part A: Polym. Chem.* **2000**, *38*, 3211.
(25) Tselikas, Y.; Iatrou, H.; Hadjichristidis, N.; Liang, K. S.; Mohanty, K.; Lohse, D. J. *J. Chem. Phys.* **1996**, *105*, 2456.
(26) Floudas, G.; Pakula, T.; Velis, G.; Sioula, S.; Hadjichristidis, N. *J. Chem. Phys.* **1998**, *108*, 6498.
(27) *Polymer Handbook, 4th Edition*; Brandrup, J., Immergut, E. H., Grulke, E. A. Eds.; Wiley-Interscience: New York, 1999.
(28) Yamakawa, H. *Modern Theory of Polymer Solutions*; Harper and Row: New York, 1971.
(29) Roovers, J.; Martin, J. E. *J. Polym. Sci. Part B: Polym. Phys.* **1989**, *27*, 2513.
(30) Schillen, K.; Brown, W.; Jonhsen, R. M. *Macromolecules* **1994**, *27*, 4825.
(31) Nakano, M.; Matsuoka, H.; Yamaoka, H.; Poppe, A.; Richter, D. *Macromolecules* **1999**, *32*, 697.
(32) Schuch, H.; Klingler, J.; Rossmanith, P.; Frechen, T.; Gerst, M.; Feldthusen, J.; Muller, A. H. E. *Macromolecules* **2000**, *33*, 1734.
(33) Schmidt, M.; Nerger, D.; Buchard, W. *Polymer* **1979**, *20*, 582.
(34) Antonietti, M.; Bremser, N.; Schmidt, M. *Macromolecules* **1990**, *23*, 3796.

MA011795C